



UNIVERSIDADE ESTADUAL DE CAMPINAS  
SISTEMA DE BIBLIOTECAS DA UNICAMP  
REPOSITÓRIO DA PRODUÇÃO CIENTÍFICA E INTELLECTUAL DA UNICAMP

**Versão do arquivo anexado / Version of attached file:**

Versão do Editor / Published Version

**Mais informações no site da editora / Further information on publisher's website:**

<https://link.springer.com/article/10.1007/s00441-010-0931-6>

**DOI: 10.1007/s00441-010-0931-6**

**Direitos autorais / Publisher's copyright statement:**

©2010 by Springer. All rights reserved.

DIRETORIA DE TRATAMENTO DA INFORMAÇÃO

Cidade Universitária Zeferino Vaz Barão Geraldo

CEP 13083-970 – Campinas SP

Fone: (19) 3521-6493

<http://www.repositorio.unicamp.br>

# Development of secondary palate requires strict regulation of ECM remodeling: sequential distribution of RECK, MMP-2, MMP-3, and MMP-9

Ana Claudia Cardoso de Oliveira Demarchi · Willian Fernando Zambuzzi ·  
Katiúcia Batista Silva Paiva · Maria das Graças da Silva-Valenzuela ·  
Fabio Dumas Nunes · Rita de Cássia Sávio Figueira · Regina Maki Sasahara ·  
Marcos Angelo Almeida Demasi · Sheila Maria Brochado Winnischofer ·  
Mari Cleide Sogayar · José Mauro Granjeiro

Received: 3 September 2009 / Accepted: 15 January 2010 / Published online: 19 February 2010  
© Springer-Verlag 2010

**Abstract** We have evaluated RECK (reversion-inducing-cysteine-rich protein with Kazal motifs), MMP-2 (matrix metalloproteinase-2), MMP-3, and MMP-9 involvement during palate development in mice by using various techniques. Immunohistochemical features revealed the distribution of RECK, MMP-2, and MMP-3 in the mesenchymal tissue and in the midline epithelial seam at embryonic day 13 (E13), MMPs-2, -3, and -9 being particularly expressed at E14 and E14.5. In contrast, RECK was weakly immunostained at these times. Involvement of MMPs was validated by measuring not only their protein

expression, but also their activity (zymograms). In situ hybridization signal (ISH) for RECK transcript was distributed in mesenchymal and epithelial regions within palatal shelves at all periods evaluated. Importantly, the results from ISH analysis were in accord with those obtained by real-time polymerase chain reaction. The expression of RECK was found to be temporally regulated, which suggested possible roles in palatal ontogeny. Taken together, our results clearly show that remodeling of the extracellular matrix is finely modulated during secondary palate development and occurs in a sequential manner.

---

Ana Claudia Cardoso de Oliveira Demarchi and Willian Fernando Zambuzzi contributed equally to this work.

---

We thank the Brazilian Funding Agencies for supporting this research: PRP-USP, CAPES (Fellowship to K.B.S.P.), FAPESP (grant no. 01/10707-7). W.F.Z. is supported by FAPESP (no. 08/53003-9), CNPq (grant nos. 350084/03-3, 475721/2003-9, and 505350/04-1), and FINEP (no. 01.04.0469.00).

---

A. C. C. de Oliveira Demarchi · W. F. Zambuzzi  
Department of Biochemistry, IB, University of Campinas,  
Campinas, SP, Brazil

K. B. S. Paiva · F. D. Nunes  
Laboratory of Molecular Pathology, Department of Oral  
Pathology, Dental School, University of São Paulo,  
São Paulo, SP, Brazil

M. d. G. da Silva-Valenzuela · R. de Cássia Sávio Figueira ·  
R. M. Sasahara · M. A. A. Demasi · S. M. B. Winnischofer ·  
M. C. Sogayar  
Department of Biochemistry, Chemistry Institute,  
University of São Paulo,  
São Paulo, SP, Brazil

M. C. Sogayar · J. M. Granjeiro  
Cell and Molecular Therapy Center, University of São Paulo,  
São Paulo, SP, Brazil

J. M. Granjeiro (✉)  
Department of Cell and Molecular Biology, Biology Institute,  
Fluminense Federal University,  
Rua Outeiro de São João Baptista, s/n, Campus do Valonguinho,  
Centro—24.020-150,  
Niterói, RJ, Brazil  
e-mail: jmgranjeiro@vm.uff.br

**Keywords** RECK · MMP-2 · MMP-3 · MMP-9 · Palate development · ECM remodeling · Mouse

## Introduction

Craniofacial anomalies comprise a significant component of morbid human birth defects. They require surgical, nutritional, dental, speech, medical, and behavioral interventions and impose a substantial economic burden (Strauss 1999). Formation of the mammalian secondary palate begins with the appearance of bilateral outgrowths from the maxillary processes; these grow and extend vertically along the sides of the tongue (Ferguson 1988). Hereafter, through alterations in the morphology of cells along the medial edge epithelia (MEE), the shelves adhere and form a single structure bisected by a layer of epithelium, known as the medial epithelial seam (MES). The MES subsequently disappears, leading to a continuous palatal shelf consisting of a mesenchymal core bounded by the nasal and oral epithelium. The mechanism by which the MES degrades to form a continuous mesenchymal palatal shelf has been a matter of intense debate. Indeed, it is fair to say that the mechanisms governing these events are obscure at best.

Extracellular matrix (ECM) turnover is clearly involved during palatogenesis events, and matrix metalloproteinases (MMPs) play a critical role during this process (Morris-Wiman et al. 1999; Mansell et al. 2000; Blavier et al. 2001; Brown et al. 2002; Shi et al. 2008). On the other hand, a novel endogenous inhibitor of MMPs has been discovered (Sasahara et al. 1999a, 1999b, 2002); products of the RECK gene (reversion-inducing-cysteine-rich protein with Kazal motifs) were first identified by inducing phenotype reversion in mice fibroblasts (NIH-3T3) transformed by Ras (v-Ki-Ras). Current work has revealed that RECK is widely expressed in normal human and mouse tissues (Nuttall et al. 2004; Takahashi et al. 1998; Accorsi-Mendonça et al. 2008; Zambuzzi et al. 2009a; Paiva et al. 2009). Thus, a temporal and spatial distribution of RECK and other MMPs occurs during remodeling, reorientation, and fusion of mice palate shelves. Interestingly, from our understanding, this is the first work to describe the involvement of RECK during palate development. Taken together, our results clearly show that ECM remodeling is finely modulated during secondary palate development and occurs in a sequential manner.

## Materials and methods

### Animals and groups

Swiss mice (*Mus musculus*) were fed *ad libitum*. All animal procedures conducted in this study received prior approval

from the local Animal Protection Committee (FOB-USP, Bauru, SP, Brazil) and were in agreement with COBEA (Colégio Brasileiro de Experimentação Animal) guidelines for animal protection. Briefly, females were kept in cages previously occupied by a male mouse to produce the Whitten effect (Whitten et al. 1968). After 4 days, the female cages were joined with those of males for 6 h during the dark cycle. Observation of the vaginal plug indicated the zero-time point (gestational day 0; E0) of the gestational period. Pregnant females were randomly grouped and killed after E13, E14, E14.5, and E15, and the palates of the embryos were carefully dissected ( $n=5$ /period).

### In situ hybridization

Briefly, samples of entire heads were fixed in freshly prepared 4% paraformaldehyde in phosphate-buffered saline (PBS) for 18 h, treated with 30% sucrose solution, frozen, and stored at  $-80^{\circ}\text{C}$ . Longitudinal serial sections (10  $\mu\text{m}$ ) were obtained in a cryostat. Endogenous peroxidase was inhibited with 6% hydrogen peroxide (MERCK, Darmsted, Germany) for 3 min at room temperature, and antigenic recovery was performed by using 10  $\mu\text{g}/\text{ml}$  proteinase K for 20 min at  $37^{\circ}\text{C}$ . Then, sections were washed in PBS-T (PBS containing 0.02% Tween-20) three times for 5 min, pre-hybridized with hybridization buffer containing 50% formamide,  $5\times$  sodium chloride-sodium citrate buffer, 50  $\mu\text{g}/\text{ml}$  yeast tRNA, and 1% SDS, and incubated for 1 h at  $50^{\circ}\text{C}$ . Afterwards, antisense and sense RNA probes were added to the hybridization buffer, and then the sections were incubated overnight at  $50^{\circ}\text{C}$ . A digoxigenin-labeled probe was used to visualize the distribution of RECK mRNA. The ribo-probe construct was synthesized by sub-cloning a 463-bp RECK cDNA fragment kindly supplied by Dr. M. Noda (Kyoto University, Kyoto, Japan). The nucleotide sequence used was as shown below:

```
5'CCGGACATGGCGAGCGTCCGGGCCCTCCCCGCG
CAGCGCGCTGCTACTTCTGCTGGCCGCGGCGG
GGGTCGCGGAGGTGACGGGGGGCCTGGCCCCGGG
CAGCGCGGGTGCTGTATGCTGTAATCATTC
AAAAGATAACCAATGTGCCGTGATGTATGTGAG
CAGATTTTCTCCTCAAAAAGTGAATCCCGA
CTGAAACATCTGTTGCAGAGAGCCCCAGAT
TATTGCCCTGAAACAATGGTTGAAATTTGG
AGTTGCATGAATTCGTCTTTGCCAGGGGTATTTAA
GAAGTCCGATGGTTGGGTTGGCTTAGGCTG
CTGTGAACTGGCTATTGGCTTGAGTGCCGACAGG
CATGCAAGCAGGCATCTTCGAAAAATGATA
TTTCCAAAGTTTGCAGGAAAGAATATGAGA
ATGCTCTTTTTCAGTTGCATTAGCAGAAAT
GAAATGGGCTCGGTGTGCTGCA 3'
```

In situ hybridization (ISH) was performed as previously described (Wu and Oh 1996) with the sonic hedgehog

(Shh) gene being used as a positive control (Nunes et al. 2007) and the sense riboprobe being used as a negative control. Color development of the hybridization signal was performed between 2–4 h.

#### Real-time polymerase chain reaction

Palates were macerated, kept in liquid nitrogen during this process, and incubated in lysis buffer (4 M guanidine isothiocyanide, 25 mM sodium citrate pH 7.0, plus 0.1 M beta-mercaptoethanol). The tissue lysate was transferred to polyalomer tubes containing 5.7 M cesium chloride and 25 mM sodium acetate, pH 5.0, and centrifuged at 164,080g for 18 h at 20°C (Chirgwin et al. 1979). The precipitated RNA was dissolved in sterile water. After spectrophotometric quantification, RNA quality was assayed in agarose gels containing 20 mM guanidine isothiocyanide. Total RNA was used as the template for cDNA synthesis in a reverse transcription reaction, which was prepared with 1 µg total RNA from dissected palate, 1 µl oligo dT 500 ng/ml (Amersham Biosciences, Sunnyvale, Calif., USA), 0.5 µl “Random Primer” (100 ng/µl), and H<sub>2</sub>O to give a final volume of 12 µl. Samples were incubated at 75°C for 10 min followed by the addition of 7 µl of a solution containing 2 µl Buffer 5× for SuperScript enzyme (Invitrogen, Carlsbad, Calif., USA), 2 µl dithiothreitol, and 0.5 µl RNase out (40 U/µl; Invitrogen). Further incubation was performed at 25°C for 10 min and 42°C for 2 min, at which time 1 µl SuperScript (200 U/µl; Invitrogen) was added. The reaction occurred during incubation at 42°C for 2 h. For enzyme inactivation, the samples were incubated at 72°C for 10 min. In order to degrade the RNA, 1 µl RNase H (5 U/µl; USB, Cleveland, Ohio, USA) was added to each tube, and the tubes were then incubated at 37°C for 30 min, followed by incubation at 72°C for 10 min to inactivate the RNase H. Samples were then diluted in 60 µl TE buffer (10 mM TRIS-HCl, pH 8.0, plus 1 mM EDTA). The primers used for gene amplification during the real-time polymerase chain reaction (PCR) were designed with PrimerExpress software (Applied Biosystems, Foster City, Calif., USA), the reaction being run on an ABI-5700 thermocycler (Applied Biosystems). Primers used for mouse RECK were (forward: 5' TGCAAGCAGGCATCTTCAA 3'; reverse: 5' AC CGAGCCCATTTTCATTTCTG 3'), and mouse D-glyceraldehyde-3-phosphate dehydrogenase (GAPDH) was used as a housekeeping gene. To quantify the product formed during the real-time PCR, the SYBR Green Dye reagent (Applied Biosystems) was used, because of its affinity with the minor groove of double-stranded DNA. After binding to double-stranded DNA, fluorescence emission of the SYBR Green Dye at 520 nm increased 100 times, enabling detection of the PCR products in real

time (Lekanne Deprez et al. 2002). Management of the thermocycler and assessment of data generated during amplification were performed by using ABA-Manager SDS software (Roche, Indianapolis, Ind., USA), which was also used to determine the primer concentrations that resulted in minimal or no primer-dimer formation, and minimal variation between pairs. All real-time PCRs were performed in duplicate, twice. As a template, 3 µl of previously synthesized cDNA, 3 µl primer (final concentration 600 nM), and 6 µl SYBR Green Dye were used. During preliminary data analysis with ABI-Manager SDS software, a threshold within the exponential stage of gene amplification was manually determined. Thus, relative quantification was used for data analysis, for each sample; the relative gene expression was determined based on the gene expression of a constitutively expressed gene (GAPDH). Calculations based on the  $2^{-\Delta\Delta Ct}$  method (Schmittgen 2001) enabled the difference in product generation of PCR to be analyzed.

#### Immunohistochemistry

Frontal-dorsal serial sections (5 µm thickness) were mounted on poly-L-lysine-coated slides. The slides were dried overnight at 37°C, the paraffin was removed in xylene, and re-hydration was achieved with consecutive ethanol washes (100%, 95%, 70%). Endogenous peroxidase was blocked in 3% hydrogen peroxide for 45 min, antigenic retrieval was performed in phosphate-citrate buffer (pH 6.0 at 96°C; P4809, Sigma-Aldrich, Mo., USA) for 20 min, and non-specific binding was blocked by incubation with 4% non-fat milk solution for 20 min, as described elsewhere (Accorsi-Mendonça et al. 2005; Menezes et al. 2006; Corotti et al. 2009; Zambuzzi et al. 2009b). Sections were incubated overnight at 4°C with polyclonal primary antibodies, namely goat anti-human MMP-2 (sc 6838), goat anti-human MMP-3 (sc 6839), goat anti-mouse MMP-9 (sc 6841), and goat anti-mouse RECK (sc 9689). The antibodies were purchased from Santa Cruz Biotechnology (Calif., USA) and used at dilutions of 1:200 (1.0 µg/ml), 1:100 (2.0 µg/ml), 1:100 (2.0 µg/ml), and 1:100 (2.0 µg/ml) in 0.1% bovine serum albumin (BSA)/PBS, respectively. Subsequently, sections were incubated in biotinylated secondary antibody (ImmunoPure rabbit anti-goat IgG [heavy + light] biotin-conjugated; Pierce, 31732) at room temperature for 1 h. Indirect immunohistochemistry was carried out by using the StreptABCComplex/horseradish peroxidase duet kit mouse/rabbit (Dakocytomation, Carpinteria, Calif., USA) for 45 min, and immunostaining was revealed by means of a chromogenic substrate mixture (DAB, 3-3'-diaminobenzidine; Dakocytomation). The sections were counterstained with Harris's hematoxylin. All rinses were performed three times in 0.1% Triton X-100 in

PBS (Merck, Darmstadt, Germany). A negative control was performed by replacement of primary antibodies with 0.1% BSA.

Human breast cancer biopsies were used as a positive control for MMP-2 and MMP-9 (Monteagudo et al. 1990), oral squamous cell carcinomas for MMP-3 (Ogbureke et al. 2007), and mouse embryos for RECK (Echizenya et al. 2005; Oh et al. 2001).

### Gel zymography

Palates were dissected by using a stereoscopic magnifying lens and frozen/kept at  $-80^{\circ}\text{C}$  until zymographic analysis, in accordance with a previously reported protocol (de Souza et al. 2000). At the moment of use, the samples were solubilized in 25% Triton X-100 and centrifuged at 45,238g, and the supernatant was transferred to another tube containing incubation buffer composed of 50 mM TRIS-HCl plus 10 mM  $\text{CaCl}_2$ , 1 mM PMSF (phenyl-methyl sulphonyl fluoride—serine-protease enzyme inhibitor), pH 7.4. The samples were then treated at  $50^{\circ}\text{C}$  for 2 h, gently shaken every 10 min, and re-centrifuged at 45,238g, when the supernatant was used for zymographic analysis. The amount of protein was determined by the Bradford methodology (Bradford 1976). Samples were diluted in non-reducing buffer (0.1 M TRIS-HCl pH 6.8, 20% glycerol, 1% SDS, 0.001% bromophenol blue). Discontinuous polyacrylamide electrophoresis containing SDS (SDS-PAGE) and 4% gelatin was conducted at  $4^{\circ}\text{C}$  and 30 mA for 8 h on a 3.8% stacking gel and 10% running gel loaded with 20  $\mu\text{g}$  protein per lane. After being resolved, the proteins were renatured by incubating the gels with 2% Triton X-100 for 1 h and re-incubating with 50 mM TRIS-HCl, 10 mM  $\text{CaCl}_2$  (pH 7.4) at  $37^{\circ}\text{C}$  for 18 h. Lastly, the gels were stained with 0.5% Coomassie Blue G 250 for 30 min and then washed in a 30% methanol and 10% glacial acetic acid solution. Gel images were obtained by scanning the gel at a resolution of 300 dpi. Analysis was conducted by using ImageTool 3 software (University of Texas Health Science Center, San Antonio, USA).

## Results

### Transient distribution of RECK transcript at studied time points

At E13, a positive hybridization signal for mRECK was observed in the palatal mesenchyme, being more evident in the midoral and medial regions (Fig. 1a, arrowheads) and in all epithelial regions, mainly in the oral region (Fig. 1a, arrow). By E14, the positive signal for mRECK had decreased in the mesenchyme medial region, being ob-

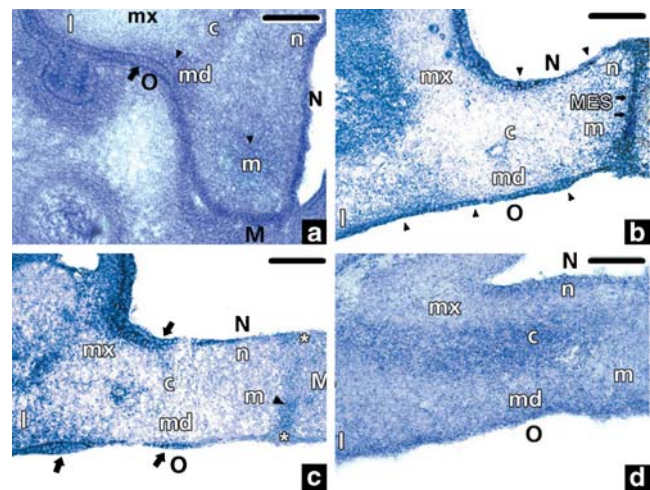


**Fig. 1** Temporal and spatial distribution of RECK transcripts during palatogenesis as revealed by in situ hybridization. **a** E13. **b** E14. **c** E14.5. **d** E15. Mesenchyme tissue is divided into regions as follows: nasal (*n*), maxillary (*mx*), medial (*m*), central (*c*), lateral (*l*), and midoral (*md*). The epithelial regions are nasal (*N*), medial (*M*) and oral (*O*). For an explanation of arrows and arrowheads, see text. Bars 30  $\mu\text{m}$  (**a–c**), 80  $\mu\text{m}$  (**d**)

served in all palatal epithelia (Fig. 1b, arrowheads) and the MES (Fig. 1b, arrows). At E14.5, a stronger mRECK signal was detected in the palatal epithelium, mainly in the oral and nasal regions (Fig. 1c, arrows), in the remaining epithelial cells within the MES (Fig. 1c, arrowhead), and in the epithelial triangle (sites of potential migration of MES cells) judging from the oral and nasal views (Fig. 1c, stars); the mRECK signal was also moderately dispersed throughout the palatal mesenchyme. On E15, a more disperse and widely spread mRECK signal was found throughout the epithelium and palatal mesenchyme, when compared with the previous period (Fig. 1d).

### Maximal level of mRECK obtained by real-time PCR after ECM remodeling and fusion of palatal shelves

In agreement with results obtained previously by ISH, real-time PCR confirmed the presence of mRECK at E13, E14, E14.5, and E15 (Fig. 2). Statistical analysis revealed a significant difference in the relative expression of mRECK between E13 and E15 and between E14 and E15.

### Dispersed RECK immunostaining expression in mesenchyme

At E13, cells immunopositive for RECK were observed along the palatal epithelium in the oral region (Fig. 3m, arrow) and were dispersed throughout the mesenchyme tissue, but this was less marked than in the ventral, medial

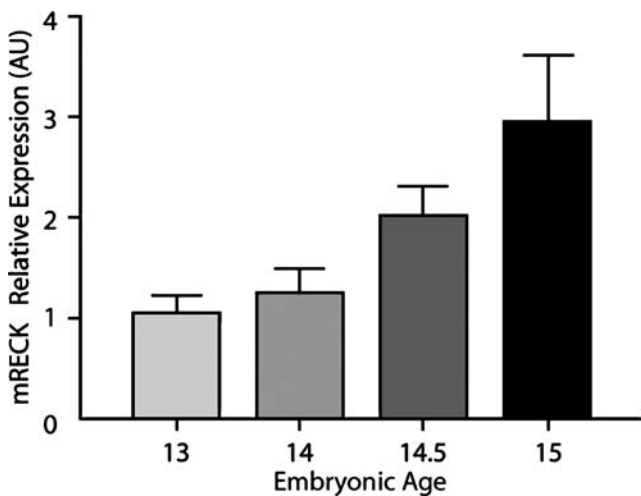


**Fig. 2** RECK mRNA expression evaluated by quantitative real-time PCR analysis. Results are expressed in arbitrary units (AU), as levels of mRNA expression relative to the expression of D-glyceraldehyde-3-phosphate dehydrogenase. Data represent the mean value of duplicates from four independent experiments for each study period. Statistical analysis was performed by using one-way analysis of variance and the Tukey multiple comparison test (GraphPad Prism software). A statistically significant difference was observed in RECK mRNA expression between periods E13 and E15 and between periods E14 and E15 ( $P < 0.05$ )

and midoral regions (Fig. 3m). At E14, RECK was observed in cells resident along epithelium, mainly in the MES (Fig. 3n, arrowhead). In the mesenchymal region, RECK expression remained disperse, including the ventral medial and midoral regions (Fig. 3n). At E14.5, RECK immunostaining in the mesenchyme appeared lower than that at the previous time points. However, in the epithelium region, the distribution pattern remained the same (Fig. 3o, arrowhead). At E15, RECK was more intensively expressed in the palatal mesenchyme than in the epithelium (Fig. 3p).

#### Presence of MMP-2 expression at all periods analyzed

At E13, some cells resident in the mesenchyme of palatal shelves in the nasal, dorsal-medial, central, and maxillary regions were immunopositive for MMP-2 (Fig. 3a). This was also true for whole epithelium surrounding the mesenchyme, mainly in the oral and medial regions (Fig. 3a, arrow). At E14 (Fig. 3b) and E14.5 (Fig. 3c), the same profile of immunostaining pattern persisted in the maxillary, medial, nasal, and central mesenchyme regions extending to the medial ventral region close of midoral region. Notably, MES cells were immunopositive (Fig. 3b, c, arrowheads). At E15, MMP-2 was observed mainly in ossification sites of the maxillary and central regions (Fig. 3d). MMP-2 was also clearly observed in the epithelial triangles (Fig. 3d, arrowheads).

#### Maximal MMP-2 activity at E14.5

Analysis of zymograms showed pro-, intermediate, and active forms of MMP-2 at all periods analyzed, with the highest activity levels being detected at E14.5 (Fig. 4a). Although statistical analysis of variance demonstrated a significant difference in the relative concentration of the forms of MMP-2 at E14.5, this might not have represented biological significance, since the maximum difference found was 20% in some cases (Fig. 4b).

#### Absence of MMP-9 on protein level at E13

At E13, MMP-9 was not immunolocalized in the mesenchyme and epithelial tissue of the secondary palate (Fig. 3i). By E14, MMP-9 was expressed in the MES (Fig. 3j, arrowheads) and ossification sites. At E14.5, MMP-9 had spread out to other mesenchyme regions, including the ventral medial close to the midoral region (Fig. 3k), whereas the remaining epithelial cells in the MES remained immunopositive in our biological model (Fig. 3k, arrowheads). By E15, MMP-9 expression had decreased, being more evident in ossification sites (Fig. 3l) and epithelial triangles (Fig. 3l, arrowheads) and in both nasal and oral aspects.

#### Maximal MMP-9 activity at E14.5

Zymogram confirmed the absence of MMP-9 activity at E13, but the levels of MMP-9 subsequently increased (Fig. 4a). A statistical analysis of variance was carried out and revealed differences mainly at E14.5.

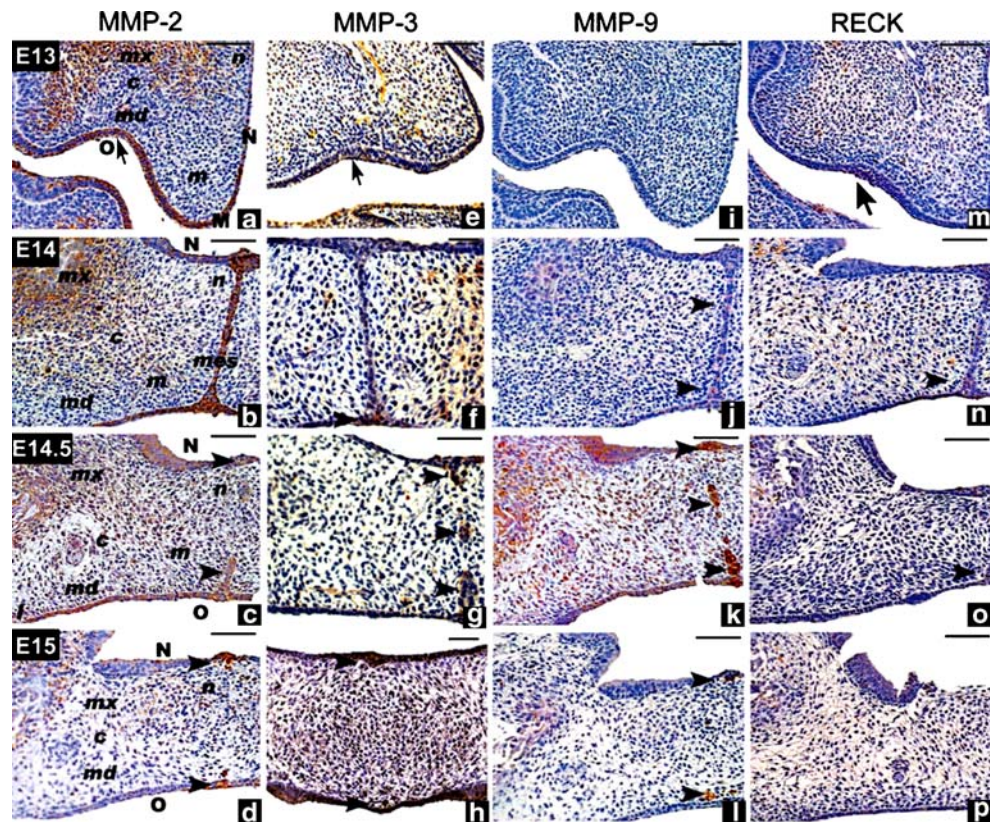
#### Expression of MMP-3 in cells resident in epithelium and mesenchyme

At E13, MMP-3 was distributed in the oral epithelium (Fig. 3e, arrow) and dispersed in all mesenchyme tissue. At E14, immunopositive cells for MMP-3 were found mainly within the MES and mesenchyme (Fig. 3f). On E14.5, the expression of MMP-3 remained in the epithelial cells located in the MES (Fig. 3g, arrowheads), and MMP-3 expression was diffuse in the mesenchyme and ossification sites (Fig. 3g). At E15, strong immunostaining for MMP-3 was observed in epithelial triangles (Fig. 3h, arrowheads) in both nasal and oral regions and was dispersed in the mesenchyme tissue (Fig. 3h).

## Discussion

Our work shows, for the first time, variations in the temporal and spatial distribution of RECK, an endogenous

**Fig. 3** Temporal and spatial distribution of RECK, MMP-2, MMP-3, and MMP-9 during palatogenesis as revealed by immunohistochemical analysis. MMP-2: **a** E13, **b** E14, **c** E14.5, **d** E15. MMP-3: **e** E13, **f** E14, **g** E14.5, **h** E15. MMP-9: **i** E13, **j** E14, **k** E14.5, **l** E15. RECK: **m** E13, **n** E14, **o** E14.5, **p** E15. The mesenchyme is divided into the following regions: nasal (*n*), maxillary (*mx*), medial (*m*), central (*c*), lateral (*l*), and midoral (*md*). The epithelial regions are nasal (*N*), medial (*M*), and oral (*O*). For an explanation of arrows and arrowheads, see text (*MES* midline epithelial seam). Bar 40  $\mu$ m (**a–e**, **g**, **i–p**), 20  $\mu$ m (**f**, **h**)



MMP-inhibitor, during secondary palate development. This distribution has been compared with the expression of MMP-2, MMP-3, and MMP-9 protein, and we suggest that, in addition to these enzymes, RECK can be related to the reorganization of the mesenchyme and epithelium of the palatal shelves and with the degradation of MES formed by contact between the MEE of each palatal shelf.

On E13, MMP-2 has been immunolocalized in the nasal, medial-dorsal, central, and maxillary regions of the palatal mesenchyme. At this stage, when remodeling of the palatal shelves occurs, all regions of the ECM are composed mainly of fibronectin, collagen I and III, and hyaluronic acid (Knudsen et al. 1985; Mansell et al. 2000; Morris-Wiman and Brinkley 1992, 1993). On continuation of the remodeling process, fibronectin and collagen III levels decrease within the medial dorsal, central, and lateral regions of palatal mesenchyme during E13 and E14. MMP-2 might play a role in the degradation of fibronectin and collagen III, providing appropriate guidance to hyaluronic-acid-rich ECM expansion. In addition, we show that a decrease occurs in the mesenchymal expression of MMP-2 during the last stages, on E14.5 and especially on E15. We believe that this is related to there being no further required expansion of the ECM during these periods, but rather only its maintenance.

On E13, MMP-2 expression has been observed in the epithelium located in the oral region surrounding the

midoral mesenchyme. This epithelium presents a different cellular organization, with higher cellular density than other epithelial regions. Bulleit and Zimmerman (1985) have reported the inhibition of palatal shelf reorientation by removal of the oral epithelium in vitro, but not by removal of the nasal epithelium, strongly suggesting the importance of the oral epithelium in the reorientation of the secondary palate. Interestingly, MMP-2 immunostaining has not been detected in the mesenchyme at the midoral and medial-ventral regions, strengthening the hypothesis of the existence of a region with higher stability; this region limits ventral expansion and therefore guides palatal shelf growth. In this sense, our zymograms have confirmed MMP-2 activity in all periods studied.

On the other hand, MMP-9 has not been detected on E13 by any of the methods employed in this study. The absence of MMP-9 in the palatal shelf at the beginning of palatogenesis and its presence in subsequent stages suggest that it is secreted by basement membrane cells and differentiated cells, such as osteoblasts and osteoclasts in osteogenic sites, as observed in the present immunohistochemical analysis and as previously reported (Blavier and Delaisse 1995; Engsig et al. 2000).

The expression of both MMP-2 and MMP-9 in the MES and in its remnants on E14, E14.5, and E15 might be related to the degradation of the ECM and basement membrane, a necessary step for palatal fusion. In turn,

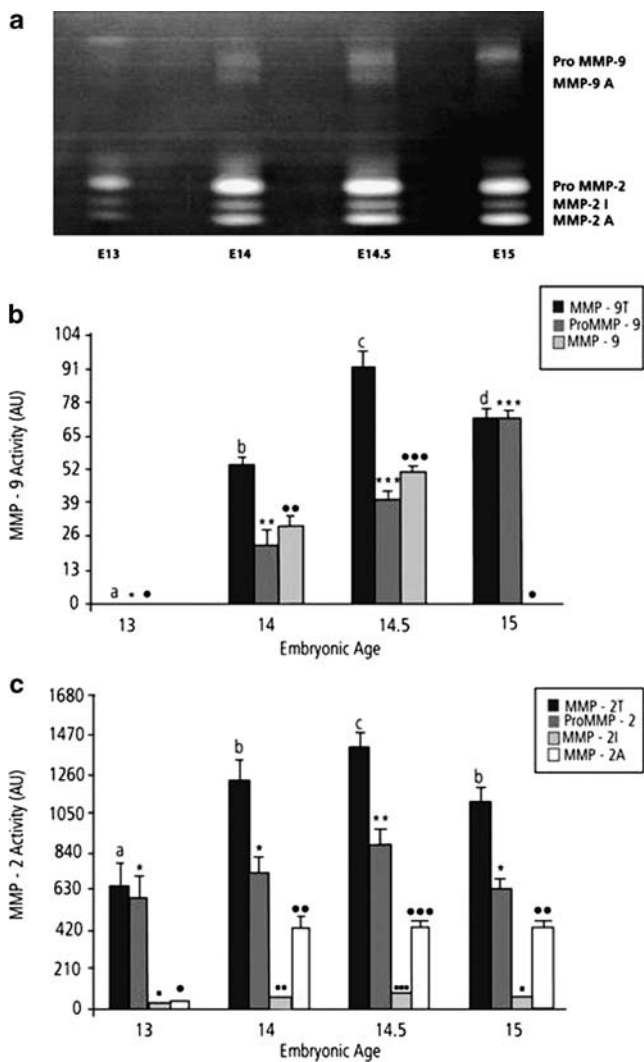


**Fig. 4** Zymographic analysis of MMP-2 and MMP-9 in dissected palates extracted at various stages of palatogenesis. **a** Scanned digitized gel images demonstrate MMP-9 in pro-active and active forms and MMP-2 in pro-active, intermediate, and active forms. **b, c** Densitometric analysis of gelatinolytic activities obtained from scanned and digitized gel images. Results are expressed in arbitrary units (AU). **b** MMP-9: statistical analysis of variance followed by Tukey test ( $P < 0.05$ ) indicates that the relative concentration of the pro- and active forms of MMP-9 are significantly different on E14.5, suggesting greater activity of this enzyme at this time point. **c** Relative concentration of various forms of MMP-2 at the studied time points. Statistical analysis of variance followed by Tukey test ( $P < 0.05$ ) indicates a significant difference in the concentration of pro-, intermediate, and active forms of MMP-2, and of total MMP-2 on E14.5 (*MMP-9T* total MMP-9, *ProMMP-9* MMP-9 pro-active form, *MMP-9A* MMP-9 active form, *MMP-2T* total MMP-2, *ProMMP-2* MMP-2 pro-active form, *MMP-2I* MMP-2 intermediary form, *MMP-2A* MMP-2 active form). Different letters or symbols denote significant differences between the bars ( $P < 0.05$ , ANOVA and Tukey's test)

MMP-3 expression is also seen in the MES, in accord with a previous study performed in vitro (Brown et al. 2002), and presents the same pattern for both gelatinases. We suggest that MMP-3 is pivotal in this process, since the

induction of its expression results in the cleavage of cadherin, the loss of epithelial phenotype, and stable epithelial-mesenchymal transformation (Lochter et al. 1997).

During palatal shelf reorganization, RECK transcripts and their product exhibit a distinctive temporal and spatial distribution. They are localized in the same regions as MMP-2, and the intensity of immunostaining is higher after ECM remodeling. Indeed, real-time PCR analysis indicates maximal mRECK expression levels on E14.5 and E15, whereas the most intense anti-RECK immunostaining has been observed on E15, results compatible with the hypothesis that RECK expression is required for the modulation of MMP-2 action in this process.

Takahashi and co-workers (1998) have reported that RECK regulates MMP-9 mechanistically by two pathways: MMP-9 suppression of cellular secretion and direct inhibition of enzyme activity. In addition, Oh and colleagues (2001) have concluded that RECK also regulates MMP-2 activity by competing with membrane-type-1 MMP (MT1-MMP) in the process of fragmentation of the ternary complex MT1-MMP/tissue inhibitor of metalloproteinases-2 (TIMP-2)/pro-MMP-2, which releases active MMP-2.

The temporal and spatial expression of MMP-2, MMP-9, and TIMPs are coincident during palatogenesis (Blavier et al. 2001), and thus interactions among these molecules probably occur. The present study has demonstrated that the expression of RECK protein is coincident with these MMPs and TIMPs, a finding that leads us to suggest that RECK also interacts with these molecules in some point during palatogenesis.

Recent studies with the gene silencing approach have confirmed that RECK modulates both MMP-2 and MT1-MMP levels (Sina et al. 2009). Micro-RNA inhibition (miR-21) has been shown to upregulate RECK and to decrease MMPs (Gabriely et al. 2008). Moreover, RECK protects some molecules from MMP catalysis (Omura et al. 2009).

Interestingly, Oh et al. (2001) have reported uterine death in the absence of *RECK* gene expression in mice. Importantly, the knockout of *TIMP* genes has little effect on the phenotype of these animals (Caterina et al. 2000; Leco et al. 2001). However, Nuttall et al. (2004) have assessed the transcript patterns of TIMPs and RECK in several organs of mouse embryo and suggest no difference between them; they have shown that RECK transcripts are present in a wide variety of mouse tissues, although RECK is expressed at most sites at a lower level than any of the four TIMPs. However, these authors do not suggest a pattern of RECK expression distinct from the TIMPs to explain this embryonic lethality.

The complex mechanisms involved in secondary palate development are clearly far from being completely under-

stood. Our findings suggest the involvement of the RECK gene in the modulation of MMP-2 and MMP-9, for which we suggest possible roles in palatal ontogeny. These findings open up another field of future study that might help us to understand these intricate mechanisms and their role in the development of craniofacial anomalies.

## References

- Accorsi-Mendonça T, Zambuzzi WF, Silva Paiva KB da, Pereira Lauris JR, Cestari TM, Taga R, Granjeiro JM (2005) Expression of metalloproteinase 2 in the cell response to porous demineralized bovine bone matrix. *J Mol Histol* 36:311–316
- Accorsi-Mendonça T, Paiva KB, Zambuzzi WF, Cestari TM, Lara VS, Sogayar MC, Taga R, Granjeiro JM (2008) Expression of matrix metalloproteinases-2 and -9 and RECK during alveolar bone regeneration in rat. *J Mol Histol* 39:201–208
- Blavier L, Delaisse JM (1995) Matrix metalloproteinases are obligatory for the migration of preosteoclasts to the developing marrow cavity of primitive long bones. *J Cell Sci* 108:3649–3659
- Blavier L, Lazaryev A, Groffen J, Heisterkamp N, DeClerck YA, Kaartinen V (2001) TGF-beta3-induced palatogenesis requires matrix metalloproteinases. *Mol Biol Cell* 12:1457–1466
- Bradford MM (1976) A rapid and sensitive method for the quantitation of microgram quantities of protein utilizing the principle of protein-dye binding. *Anal Biochem* 72:248–254
- Brown NL, Yarram SJ, Mansell JP, Sandy JR (2002) Matrix metalloproteinases have a role in palatogenesis. *J Dent Res* 81:826–830
- Bulleit RF, Zimmerman EF (1985) The influence of the epithelium on palate shelf reorientation. *J Embryol Exp Morphol* 88:265–279
- Caterina JJ, Yamada S, Caterina NC, Longenecker G, Holmback K, Shi J, Yermovsky AE, Engler JA, Birkedal-Hansen H (2000) Inactivating mutation of the mouse tissue inhibitor of metalloproteinases-2 (Timp-2) gene alters proMMP-2 activation. *J Biol Chem* 275:26416–26422
- Chirgwin JM, Przybyla AE, MacDonald RJ, Rutter WJ (1979) Isolation of biologically active ribonucleic acid from sources enriched in ribonuclease. *Biochemistry* 18:5294–5299
- Corotti MV, Zambuzzi WF, Paiva KB, Menezes R, Pinto LC, Lara VS, Granjeiro JM (2009) Immunolocalization of matrix metalloproteinases-2 and -9 during apical periodontitis development. *Arch Oral Biol* 54:764–771
- de Souza AP, Gerlach RF, Line SR (2000) Inhibition of human gingival gelatinases (MMP-2 and MMP-9) by metal salts. *Dent Mater* 16:103–108
- Echizenya M, Kondo S, Takahashi R, Oh J, Kawashima S, Kitayama H, Takahashi C, Noda M (2005) The membrane-anchored MMP-regulator RECK is a target of myogenic regulatory factors. *Oncogene* 24:5850–5857
- Engsig MT, Chen QJ, Vu TH, Pedersen AC, Therkildsen B, Lund LR, Henriksen K, Lenhard T, Foged NT, Werb Z, Delaisse JM (2000) Matrix metalloproteinase 9 and vascular endothelial growth factor are essential for osteoclast recruitment into developing long bones. *J Cell Biol* 151:879–889
- Ferguson MW (1988) Palate development. *Development* 103:41–60
- Gabriely G, Wurdinger T, Kesari S, Esau CC, Burchard J, Linsley PS, Krichevsky AM (2008) MicroRNA 21 promotes glioma invasion by targeting matrix metalloproteinase regulators. *Mol Cell Biol* 28:5369–5380
- Knudsen TB, Bulleit RF, Zimmerman EF (1985) Histochemical localization of glycosaminoglycans during morphogenesis of the secondary palate in mice. *Anat Embryol (Berl)* 173:137–142
- Leco KJ, Waterhouse P, Sanchez OH, Gowing KL, Poole AR, Wakeham A, Mak TW, Khokha R (2001) Spontaneous air space enlargement in the lungs of mice lacking tissue inhibitor of metalloproteinases-3 (TIMP-3). *J Clin Invest* 108:817–829
- Lekanne Deprez RH, Fijnvandraat AC, Ruijter JM, Moorman AF (2002) Sensitivity and accuracy of quantitative real-time polymerase chain reaction using SYBR green I depends on cDNA synthesis conditions. *Anal Biochem* 307:63–69
- Lochter A, Galosy S, Muschler J, Freedman N, Werb Z, Bissell MJ (1997) Matrix metalloproteinase stromelysin-1 triggers a cascade of molecular alterations that leads to stable epithelial-to-mesenchymal conversion and a premalignant phenotype in mammary epithelial cells. *J Cell Biol* 139:1861–1872
- Mansell JP, Kerrigan J, McGill J, Bailey J, TeKoppele J, Sandy JR (2000) Temporal changes in collagen composition and metabolism during rodent palatogenesis. *Mech Ageing Dev* 119:49–62
- Menezes R, Bramante CM, da Silva Paiva KB, Letra A, Carneiro E, Fernando Zambuzzi W, Granjeiro JM (2006) Receptor activator NFkappaB-ligand and osteoprotegerin protein expression in human periapical cysts and granulomas. *Oral Surg Oral Med Oral Pathol Oral Radiol Endod* 102:404–409
- Monteagudo C, Merino MJ, San-Juan J, Liotta LA, Stetler-Stevenson WG (1990) Immunohistochemical distribution of type IV collagenase in normal, benign, and malignant breast tissue. *Am J Pathol* 136:585–592
- Morris-Wiman J, Brinkley L (1992) An extracellular matrix infrastructure provides support for murine secondary palatal shelf remodelling. *Anat Rec* 234:575–586
- Morris-Wiman J, Brinkley L (1993) Rapid changes in the extracellular matrix accompany in vitro palatal shelf remodeling. *Anat Embryol (Berl)* 188:75–85
- Morris-Wiman J, Du Y, Brinkley L (1999) Occurrence and temporal variation in matrix metalloproteinases and their inhibitors during murine secondary palatal morphogenesis. *J Craniofac Genet Dev Biol* 19:201–212
- Nunes FD, Valenzuela MG, Rodini CO, Massironi SM, Ko GM (2007) Localization of Bmp-4, Shh and Wnt-5a transcripts during early mice tooth development by in situ hybridization. *Braz Oral Res* 21:127–133
- Nuttall RK, Sampieri CL, Pennington CJ, Gill SE, Schultz GA, Edwards DR (2004) Expression analysis of the entire MMP and TIMP gene families during mouse tissue development. *FEBS Lett* 563:129–134
- Ogbureke KU, Nikitakis NG, Warburton G, Ord RA, Sauk JJ, Waller JL, Fisher LW (2007) Up-regulation of SIBLING proteins and correlation with cognate MMP expression in oral cancer. *Oral Oncol* 43:920–932
- Oh J, Takahashi R, Kondo S, Mizoguchi A, Adachi E, Sasahara RM, Nishimura S, Imamura Y, Kitayama H, Alexander DB, Ide C, Horan TP, Arakawa T, Yoshida H, Nishikawa S, Itoh Y, Seiki M, Itoharu S, Takahashi C, Noda M (2001) The membrane-anchored MMP inhibitor RECK is a key regulator of extracellular matrix integrity and angiogenesis. *Cell* 107:789–800
- Omura A, Matsuzaki T, Mio K, Ogura T, Yamamoto M, Fujita A, Okawa K, Kitayama H, Takahashi C, Sato C, Noda M (2009) RECK forms cowbell-shaped dimers and inhibits matrix metalloproteinase-catalyzed cleavage of fibronectin. *J Biol Chem* 284:3461–3469
- Paiva KB, Zambuzzi WF, Accorsi-Mendonça T, Taga R, Nunes FD, Sogayar MC, Granjeiro JM (2009) Rat forming incisor requires a rigorous ECM remodeling modulated by MMP/RECK balance. *J Mol Histol* 40:201–207
- Sasahara RM, Takahashi C, Noda M (1999a) Involvement of the Sp1 site in ras-mediated downregulation of the RECK metastasis suppressor gene. *Biochem Biophys Res Commun* 264:668–675

- Sasahara RM, Takahashi C, Sogayar MC, Noda M (1999b) Oncogene-mediated downregulation of RECK, a novel transformation suppressor gene. *Braz J Med Biol Res* 32:891–895
- Sasahara RM, Brochado SM, Takahashi C, Oh J, Maria-Engler SS, Granjeiro JM, Noda M, Sogayar MC (2002) Transcriptional control of the RECK metastasis/angiogenesis suppressor gene. *Cancer Detect Prev* 26:435–443
- Schmittgen TD (2001) Real-time quantitative PCR. *Methods* 25:383–385
- Shi J, Son MY, Yamada S, Szabova L, Kahan S, Chrysovergis K, Wolf L, Surmak A, Holmbeck K (2008) Membrane-type MMPs enable extracellular matrix permissiveness and mesenchymal cell proliferation during embryogenesis. *Dev Biol* 313:196–209
- Sina A, Lord-Dufour S, Annabi B (2009) Cell-based evidence for aminopeptidase N/CD13 inhibitor actinonin targeting of MT1-MMP-mediated proMMP-2 activation. *Cancer Lett* 279:171–176
- Strauss RP (1999) The organization and delivery of craniofacial health services: the state of the art. *Cleft Palate Craniofac J* 36:189–195
- Takahashi C, Sheng Z, Horan TP, Kitayama H, Maki M, Hitomi K, Kitaura Y, Takai S, Sasahara RM, Horimoto A, Ikawa Y, Ratzkin BJ, Arakawa T, Noda M (1998) Regulation of matrix metalloproteinase-9 and inhibition of tumor invasion by the membrane-anchored glycoprotein RECK. *Proc Natl Acad Sci USA* 95:13221–13226
- Whitten WK, Bronson FH, Greenstein JA (1968) Estrus-inducing pheromone of male mice: transport by movement of air. *Science* 161:584–585
- Wu DK, Oh SH (1996) Sensory organ generation in the chick inner ear. *J Neurosci* 16:6454–6462
- Zambuzzi WF, Yano CL, Cavagis AD, Peppelenbosch MP, Granjeiro JM, Ferreira CV (2009a) Ascorbate-induced osteoblast differentiation recruits distinct MMP-inhibitors: RECK and TIMP-2. *Mol Cell Biochem* 322:143–150
- Zambuzzi WF, Paiva KB, Batista AC, Lara VS, Granjeiro JM (2009b) Immunohistochemical approach reveals involvement of inducible nitric oxide synthase in rat late development. *J Mol Histol* 40:235–240